

THE BIPOLAR OPTICAL OUTFLOW ASSOCIATED WITH PV CEPHEI

MERCEDES GOMEZ¹Observatorio Astronómico, Laprida 854, 5000 Córdoba, Argentina
Electronic mail: mercedes@oac.uncor.edu; mgomez@cfa.harvard.edu

SCOTT J. KENYON

Harvard-Smithsonian Center for Astrophysics, 60 Garden Street, Cambridge, Massachusetts 02138
Electronic mail: skenyon@cfa.harvard.eduBARBARA A. WHITNEY²Space Science and Engineering Center, University of Wisconsin, 1225 West Dayton Street, Madison, Wisconsin 54706
Electronic mail: whitneyb@admin.uwex.edu

Received 1997 January 10; revised 1997 March 31

ABSTRACT

We describe deep $10' \times 19'$ CCD images of the bipolar [S II] jet emanating from the Herbig Ae/Be star PV Cephei. The ~ 2.3 pc long jet exhibits a clear S-shaped morphology and lies within the lobes of the molecular outflow. The 23 HH knots—including 21 new detections—suggest an intermittent outflow with major eruptions every ~ 2000 yr. We model the morphology of the optical outflow with a simple precessing jet; our preferred model has a large inclination to the line-of-sight, $i \sim 80^\circ$; an opening angle for the precession axis, $\theta \sim 45^\circ$; and a modest precession period of ~ 8300 yr. The close association of optical and radio outflows—together with our simple dynamical jet model—is consistent with Masson & Chernin's (1993, *ApJ*, 414, 230) picture where a precessing optical jet carves out cavities in an infalling envelope and drives a molecular outflow. © 1997 American Astronomical Society. [S0004-6256(97)01707-X]

1. INTRODUCTION

PV Cephei is a Herbig Ae/Be pre-main-sequence star associated with a bright *IRAS* source (20453+6746; Cohen *et al.* 1981; see also Hamann & Persson 1992a; 1992b; Thé *et al.* 1994; Mundt & Ray 1994; Ray 1994). The spectral classification is uncertain. Cohen *et al.* (1981) derived a spectral range of B5–F2; the Herbig & Bell (1988) and Thé *et al.* (1994) catalogs classify it as Aep+shell. In addition to a strong stellar continuum, the PV Cep optical spectrum shows variable H α , Fe II, [Fe II], Ca II, Fe I, Mg I, [O I], and [S II] emission line (Cohen *et al.* 1981; Hamann & Persson 1992a). H α is particularly outstanding with a strong redshifted emission and a deep variable P Cygni absorption (Cohen *et al.* 1981; Neckel *et al.* 1987). The spectral energy distribution (νF_ν) is roughly constant from 0.5 to 100 μm indicating that most of the bolometric luminosity comes from the infrared (Hamann & Persson 1992b; Hartmann *et al.* 1993a). This star also shows erratic photometric and spectroscopic change with several magnitude variations in brightness on time scales of months to years (Cohen 1977; Cohen *et al.* 1981; Scarrott *et al.* 1991).

PV Cep is surrounded by an optical reflection nebula (GM 29, Gyul'budagyan & Magakyan 1977; RNO 125, Cohen 1980) that has undergone dramatic changes in the past four

decades (Cohen *et al.* 1981; Neckel & Staude 1984; Neckel *et al.* 1987; Scarrott *et al.* 1991). The nebula is hardly detectable at 2 μm (Hodapp 1994; Li *et al.* 1994). On 1952 POSS plates, the optical nebulosity has a linear, streak-like shape. By 1976, a faint cometary nebulosity replaced the streak (Cohen 1977; Gyul'budagyan *et al.* 1977). The streak, roughly coincident with the eastern edge of the fan-like nebula, intermittently reappeared until 1989 (cf. Scarrott *et al.* 1991). Deep *I* band CCD observations (Scarrott *et al.* 1986; Neckel *et al.* 1987; Levreault & Opal 1987) show that the nebula has a biconical or hourglass shape. The northern lobe (the cometary or fan-shape optical nebula—GM 29, RNO 125—) is visible on the POSS plates and the southern lobe (the counter fan) is obscured by $A_V \sim 4.8$ mag (see Levreault & Opal 1987).

Levreault (1984) found an asymmetric bipolar CO outflow associated with PV Cep. Assuming a distance of 500 pc (Cohen *et al.* 1981), the approaching blue lobe extends for ~ 1.5 pc; the red lobe spans ~ 0.5 pc (see also Levreault 1988). Anglada *et al.* (1992) reported the detection of an unresolved radio continuum source (at 3.4 cm) coinciding with the position of the optical star. Carr (1990) found Br γ and H $_{2\nu=1-0S(1)}$ emission in a near-infrared spectrum of PV Cep. Greene & Lada (1996) found additional Pa β emission on more recent spectra at 1.15–2.42 μm . Hamann *et al.* (1994) detected narrow blueshifted high-velocity lines of [Fe II] 1.53 and 1.63 μm . These authors concluded that the [Fe II] line profiles (FWHM/ $V_c \sim 0.14$, V_c is the line centroid velocity) require collimated outflows or conical winds

¹Gemini Fellow at Harvard-Smithsonian Center for Astrophysics.²Present address: Wisconsin Small Business Development Center, 432 N. Lake St., Madison, WI 53706.

TABLE 1. PV Cep: Observations.

Field Center $\alpha(2000.0), \delta(2000.0)$	Date	Time _[S II] sec.	Time _{cont} sec.
20 ^h 45 ^m 54 ^s , 67° 57' 36"	6-Nov 93	2400 (3)	300 (3)
20 ^h 45 ^m 54 ^s , 67° 57' 36"	8-Nov 93	3600 (4)	480 (4)
20 ^h 45 ^m 25 ^s , 68° 02' 03"	27-Oct 94	3600 (3)	600 (3)
20 ^h 45 ^m 54 ^s , 67° 57' 37"	28-Oct 94	1200 (1)	180 (1)
20 ^h 46 ^m 07 ^s , 67° 53' 02"	28-Oct 94	2400 (2)	540 (3)

Notes. — Time is the total integration time in the [S II] filter and nearby continuum (cont) filter; number of frames is in parentheses.

with full opening angles of $\sim 30^\circ$ suggesting that the central star may be associated with an optical jet. Inside the blue-shifted CO lobe, Neckel *et al.* (1987) detected (in [O I], [S II], and H α) two low excitation narrow HH emission regions 20" and 50" north of PV Cep, respectively. Reipurth's (1994) HH catalog identifies these central objects as HH 215.

In view of the common characteristics of PV Cephei and other young stellar objects associated with jet/HH emissions (highly collimated stellar winds, bipolar molecular outflows, low excitation HH emissions within a biconical nebula, and spectroscopic and photometric variable central star) we suspected this star to be the driving source of an optical outflow. We imaged in [S II] the complete extent of the CO outflow and found that PV Cep is associated with an optical bipolar outflow composed of numerous HH/jet emissions in a field of view of $\sim 10' \times 19'$. The axes of the optical and molecular flows and the optical nebula are roughly coincident. The total extent of the optical flow is $\sim 16'$ or 2.3 pc. The observed jet lengths typically range from 0.1 to 0.6 pc for the Herbig Ae/Be stars; thus this is one of the largest optical outflows known associated with these intermediate-mass pre-main-sequence objects (see Mundt & Ray 1994). The large extent of the PV Cep HH flow was independently discovered and described by Reipurth *et al.* (1997).

In the following sections we show the [S II] images and give coordinates and differential magnitudes for the 23 HH/jet objects, 21 of which are new detections. The angle swept by the detected [S II] emissions, probably produced during eruption events of the central source, is consistent with models where precessing jets carve bipolar cavities in envelopes and drive molecular flows (Masson & Chernin 1993; Raga *et al.* 1993b; Raga & Biro 1993; Chernin & Masson 1995; Biro *et al.* 1995).

2. OBSERVATIONS AND ANALYSIS

We acquired [S II] and continuum images of PV Cep through light clouds in 1993 October and 1994 November with the 1024 \times 1024 CCD camera on the 1.2 m telescope at the Fred L. Whipple Observatory on Mt. Hopkins, Arizona. This camera provides a large field of view, 10' \times 10', with a plate scale of 0.65" per pixel. The FWHM of a point source is typically $\sim 2''$. The [S II] filter is centered at 6732 Å and has a FWHM of 54 Å. The nearby continuum filter has a central wavelength of 6968 Å and a FWHM of 350 Å. Table 1 shows the observing log.

The seven images taken in 1993 were mostly centered on PV Cep. We offset the telescope $\sim 30''$ E-W between the

frames to allow for the removal of bad pixels. These data show [S II] knots lying $\sim 6' - 7'$ away from the central star at the edge of the field (see Table 2). We returned in 1994 to obtain additional frames with PV Cep located close to the southern and northern edge of this field (see Table 1). The field of view for this sequence is $\sim 10' \times 19'$ roughly centered on the star and covers the total extent of the CO bipolar flow (see Levreault 1984, 1988). For each telescope position, we obtained both an [S II] and a continuum frame (Table 1).

Gómez *et al.* (1997) describe our IRAF-based data reduction in detail. Briefly, we took 5–10 bias and dome flats (in each filter) at the beginning and end of each night. We produced final object frames by subtracting the bias level, dividing by the appropriately normalized flatfields, and then subtracting the sky background from each image. We recentered and median-filtered multiple exposures taken at different positions and scaled the fluxes of field stars on the continuum images to have similar fluxes as on the [S II] images. To make the color images (see Figs. 2 and 3), we assigned the [S II] frame to the red plane, and the nearby-continuum image to both the blue and green planes using the IRAF task IMSTACK.

The shape of the nebulosity changed between 1993 and 1994, as shown in Fig. 1. Both the star and the nebula also faded by ~ 1 mag relative to nearby stars. In 1993 the nebula showed a V shape; the 1994 data indicate an arrow shape with one end of arrow-head pointing roughly to the N and the other to the NW (see Fig. 1). The N lobe is brighter (by ~ 1.6 mag) than the NW, suggesting that the linear streak might be reappearing again. Probably in 1994 we caught the star mid-way between the fan-shape and the linear streak states (cf. Scarrott *et al.* 1991), though the linear streak, in previous images, usually appears tilted by $\sim 15^\circ$ E of N. The continuum and the [S II] images are practically identical to each other. The southern lobe of the biconical nebula is visible in Fig. 2 (Plate 22).

To improve the contrast of faint [S II] emission, we combined data from different runs into a single image. Figure 2 shows a three-color image covering $\sim 3' \times 3'$ centered on PV Cep. The northern lobe of the nebula appears in white and the southern in blue. The [S II] emission within or close to the nebula is in red. Figure 3 (Plate 23) is a 10' \times 19' [S II] mosaic with the continuum subtracted. Reipurth *et al.* (1997) assign the designation HH 315 to the large-scale optical flow associated with PV Cep. They also note that HH 315 and HH 215, the inner group of knots (see also Neckel *et al.* 1987), form a single giant flow that for convenience they refer to as the HH 315 flow. We follow their convention in this paper. Figure 4 shows a schematic representation of the relative positions of the optical and the molecular outflows. We identify 23 [S II] knots located at different distances and directions from PV Cep. The distances range from 18" (~ 0.04 pc) to 8.5" (~ 1.2 pc). The northern knots define a full opening angle of $\sim 17^\circ$ and the southern [S II] emissions an opening angle of $\sim 11^\circ$.

Table 2 lists the coordinates, differential magnitudes in [S II], position angles, and distances from the central star for the HH/jet emissions flow detected in our images. We derived coordinates with respect to ~ 50 nearby stars on a digi-

TABLE 2. The HH 315 flow: Coordinates and differential magnitudes.

Object	$\alpha(2000.0)$ h:m:s	$\delta(2000.0)$ °:′:″	Δm	Area(″) ²	$\Delta m(4'')$	$\Delta m(2'')$	$\langle S / N \rangle$	d(to PV Cep) pc	θ degree
Knot C1	20:45:01.5	68:04:31	4.4	62	4.7	5.9	2.5	1.24	-35.9
Knot C2	20:45:03.9	68:04:30	3.5	35	3.4	4.0	8	1.22	-34.6
Knot C3	20:45:04.7	68:04:47	4.5	49	4.5	5.5	3	1.24	-33.1
Knot C4	20:45:06.3	68:04:50	3.2	142	4.0	5.0	5	1.24	-32.1
Knot C5	20:45:17.6	68:04:52	3.4	271	4.6	5.7	2.5	1.17	-25.6
Knot B8	20:45:24.5	68:04:05	3.3	323	4.0	4.9	5	1.02	-23.6
Knot B7	20:45:32.0	68:03:57	4.5	84	5.2	6.0	2	0.97	-18.6
Knot B1-6	20:45:33.6	68:03:25	2.7	900	2.7	3.7	16	0.89	-18.8
Knot A1	20:45:38.4	68:00:54	4.5	106	5.2	6.3	2.5	0.52	-24.9
HH 215(1)	20:45:55.0	67:58:31	5.9	36	5.9	6.3	4	0.13	+1.9
Knot D1-2	20:46:06.8	67:54:14	4.5	86	4.7	5.4	2.5	0.53	+160.3
Knot E2	20:46:26.7	67:52:10	3.4	130	3.8	4.5	4	0.92	+150.6
Knot E1	20:46:28.8	67:52:20	3.6	121	4.0	4.9	3.5	0.92	+148.2
Knot E7	20:46:35.3	67:52:06	4.0	81	4.3	5.0	3	0.99	+144.9
Knot E8	20:46:37.1	67:52:11	3.7	72	3.9	4.5	3.5	1.00	+143.4
Knot E6	20:46:35.3	67:51:51	4.3	111	4.6	5.3	2.5	1.02	+146.1
Knot E3	20:46:27.5	67:51:05	4.3	113	4.9	5.5	2.5	1.07	+154.2
Knot E5	20:46:29.3	67:51:06	4.9	115	5.6	6.2	1.5	1.07	+152.9
Knot E4	20:46:29.4	67:50:52	4.2	286	5.1	5.9	2	1.11	+153.7
Inside the Nebula									
HH 215(5)	20:45:53.4	67:58:15	6.8	22	6.5	7.0	2	0.09	-11.3
HH 215(4)	20:45:53.7	67:58:06	6.7	20	6.6	6.8	2	0.07	-11.2
HH 215(3)	20:45:54.5	67:58:01	5.5	51	5.8	6.4	3	0.05	-3.0
HH 215(2)	20:45:55.3	67:57:54	6.1	33	5.7	6.4	3	0.04	+12.5
Field Star	20:45:33.0	68:04:09

Note. — θ is the position angle measured positive E of N and negative W of N. — The signal-to-noise (S/N) is the ratio of the average counts per pixel to the sky (background).

tized version of the POSS.³ Our coordinates have a precision of $\sim 2''$. The differential magnitudes in [S II] are relative to a field star listed at the end of Table 2. The magnitudes in Table 1 account for the differences in total integration time between various subfields of the complete mosaic (see Table 1). The S/N column gives a very rough estimate of the relative brightness of the knots in our mosaic with respect to an average background (sky).

Figures 5(a), 5(b), 5(c) show detailed contour maps for the subtracted ([S II]—continuum) images. The optical outflow, HH 315, consists of several major [S II] condensations identified as knots A, B, C, etc. and many individual knots such as knots C1, C2, C3, or those inside knot B for example. For the designation of the new HH knots we follow Reipurth *et al.*'s (1997) notation as mentioned above. The minor blobs do not lie along a straight line but appear to wiggle inside the major condensations. Knot C shows a curving shape; knot B is the brightest. Four knots [HH 215 (2), (3), (4), (5)] lie inside the nebula and are only visible in the

subtracted image. Knots HH 215(1) and HH 215(2)–(4) (see Figs. 2 and 3) are located roughly at the same distance from the star as those detected spectroscopically by Neckel *et al.* (1987).

The different HH knots appear to trace a roughly sinusoidal path with the counter-jet emission located south of the source. Table 2 shows the change in the position angles (or

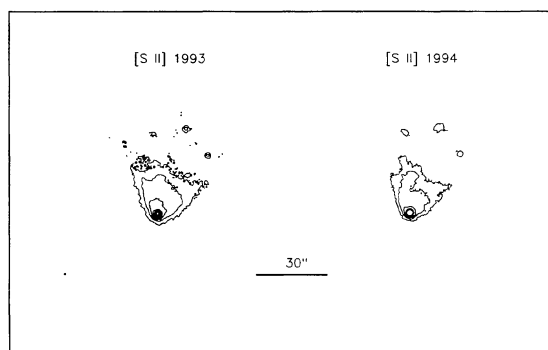


FIG. 1. The contour plot for the [S II] images for the optical nebula associated with PV Cephei corresponding to the 1993 and 1994 observations. North is up and east is left.

³The compressed digital form of the POSS plates were produced at the Space Telescope Institute under US Government grant NAG W-2166, with permission from the California Institute of Technology and the National Geographic Society.

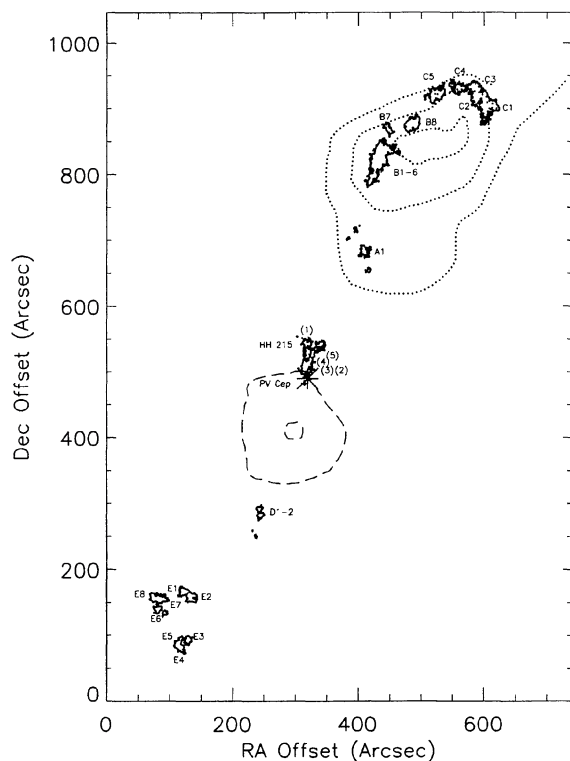


FIG. 4. Schematic representation of the relative positions of the [S II] knots (see Table 2) and the molecular outflow measured by Levreault (1984). With dotted line the figure shows the blueshifted CO emission and the dashed contours the redshifted molecular flow. The big asterisk indicates the position of the central star (PV Cephei). North is up and east is left.

direction) between consecutive knots. The starred symbols in Fig. 6 indicate the offset positions of the HH condensations with respect to the central source (the cross). In this figure we include the offset positions of five additional new HH objects (open circles) kindly provided by Dr. Bo Reipurth (Reipurth *et al.* 1997). These knots, identified as F1–5 in Reipurth *et al.*'s paper, lie outside our field.

The HH 315 S-shaped morphology is observed in other pre-main-sequences stars, including HH 46/47 (Reipurth & Heathcote 1991), HH 80–81 (Martí *et al.* 1993), HH 34 (Bally & Devine 1994, see also Reipurth & Heathcote 1992), L1228A/HH 199 (Bally *et al.* 1995), and HH 333 (Bally *et al.* 1996b). Precessing jets can explain helical or sinusoidal patterns in the optical outflows (Lightfoot & Glencross 1986; Reipurth & Heathcote 1991, 1992; Martí *et al.* 1993; Raga *et al.* 1993b; Bally & Devine 1994; Curiel *et al.* 1994; Bally *et al.* 1995; Gueth *et al.* 1996; Bally *et al.* 1996a, 1996b), but none of the sources have been modeled in detail.

As an initial dynamical model for the HH 315 outflow, we consider a simple, nonrelativistic precessing jet. Hjellming & Johnston (1981) and Grower *et al.* (1982) developed this model for relativistic jets in SS 433 and active galactic nuclei; Hollis & Michalitsianos (1993) applied the nonrelativistic case to the long period symbiotic binary R Aquarii. In these models, the jet axis precesses on the surface of a cone with opening angle, θ , inclined at an angle, i , relative to the line of sight. The jet has a constant ejection velocity, v , and

a constant precession velocity, ω . For a standard jet velocity of 200 km s^{-1} (cf. Reipurth & Cernicharo 1995), the jet length of 1.4 pc implies a dynamical time of ~ 6800 yr and a precession velocity of $\sim 1.5'/\text{yr}$. This jet length includes the group of knots ‘‘F’’ that lies outside our field of view (see Fig. 6 and Reipurth *et al.* 1997).

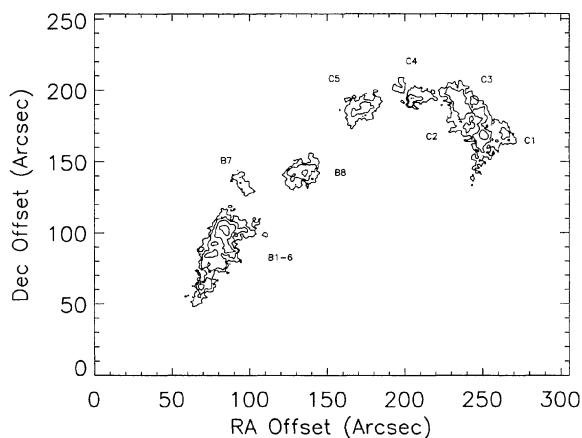
We construct a grid of model outflows for the precessing jet with $\theta=0^\circ\text{--}90^\circ$ and $i=0^\circ\text{--}90^\circ$. Model jets with $\theta=15^\circ\text{--}25^\circ$ and $i=70^\circ\text{--}90^\circ$ produce outflows that resemble our observations. The solid line in Fig. 6 shows an example for $i=80^\circ$ and $\theta=22.5^\circ$. The position angle of the precession axis, ϕ , is -36.5° . This model has a dynamical time of 8300 yr, slightly longer than the dynamical time for a straight jet with no precession. The simple model predicts a continuous jet; our data require major episodic ejections on time scales of ~ 2000 yr as we discuss in the next section.

Several other observations support this simple jet model for HH 315. The morphology of the molecular outflow—with blue and red lobes well separated on the sky—supports an edge-on geometry (Levreault 1984, 1988). The opening angle of the fan-shaped nebula, $\sim 60^\circ$, is safely larger than the full opening angle of the jet, $\sim 30^\circ$, as deduced from near-IR line profiles (Hamann *et al.* 1994) or $\sim 45^\circ$ as derived from our simple jet model. In our model, the ‘‘best’’ jet opening angle increases from $\sim 30^\circ$ at $i=70^\circ$ to $\sim 50^\circ$ at $i=90^\circ$. We can thus reconcile the near-IR line profiles and the optical jet morphology for $i\sim 70^\circ$. The opening angle of the nebular is larger than the opening angle of the HH 315 flow even for $i=90^\circ$.

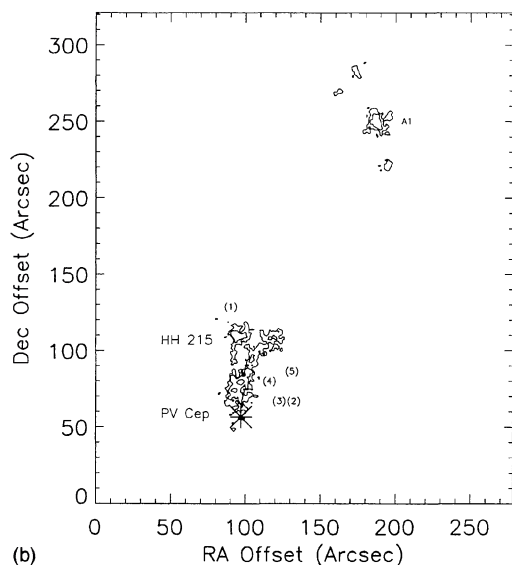
3. DISCUSSION

In recent years, several studies have suggested a clear casual connection between optical jets and molecular outflows. In this new picture, a jet or well-collimated stellar wind from the central star-disk system transfers momentum into the surrounding cloud to accelerate large-scale molecular flows (Masson & Chernin 1993; Raga & Cabrit 1993; Raga *et al.* 1993a; Königl & Ruden 1993; Adams & Lin 1993; Stahler 1994; Chernin & Masson 1995). If the jet axis slowly changes direction, the opening angle of the molecular outflow increases with time (cf. Chernin & Masson 1995). A precessing jet axis produces a helical flow that appears as a sinusoidal ‘‘meandering’’ jet projected on the sky (cf. Lightfoot & Glencross 1986; Raga *et al.* 1993b; Gueth *et al.* 1996).

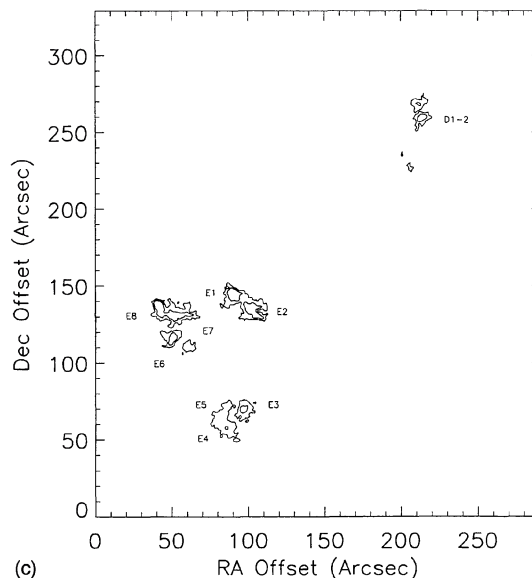
The observations of PV Cephei are consistent with this picture. Figure 4 shows the molecular and optical flows associated with this young star. The extent of the NW optical flow (~ 1.2 pc) roughly coincides with the far end of the blueshifted CO flow. We detect some apparently fainter [S II] emissions in the SE optical flow that extend farther away (~ 1.1 pc) than the ‘‘end’’ of the redshifted CO flow (~ 0.5 pc). A highly variable biconical nebula surrounds the central source (see Fig. 2). The northern lobe emerges from the edge of the cloud (see Plate 1 in Gledhill *et al.* 1987) and resemble the fan-shaped nebula observed in many other pre-main-sequences stars (cf. Neckel & Staude 1984; Bastien & Ménard 1990, and references therein). The southern lobe lies



(a)



(b)



(c)

FIG. 5. (a), (b), (c) The contour plot for the [S II]—continuum image. We divided the mosaic image of the Fig. 3 in three portions to be able to identify each of the knots and show the fine structure of the [S II] emission. Intensity contours in these figures are spaced at 1 mag intervals. The big asterisk indicates the position of the central star (PV Cephei) in (b). North is up and east is left.

embedded in the cloud material and is heavily extinguished (Levreault & Opal 1987; Fig. 2). The wide opening angle of the nebula, $\sim 60^\circ$, is comparable to the opening angle of the molecular outflow and larger than the opening angle of the optical outflow.

The morphological differences between the blue and the red molecular outflow lobes (see Fig. 4) probably originate in the cloud geometry. The red lobe of the outflow propagates into the cloud and encounters denser material than the blue lobe that appears to be flowing out of the cloud. Levreault (1984) estimated a factor of 10 difference in the cloud density from the south-east (red) to the north-west (blue) ^{13}CO lobes. This difference roughly corresponds to a gradient of $A_V \sim 4-6$ mag across the molecular outflow (Dickman 1978; Savage & Mathis 1979; Frerking *et al.* 1982; Duvert *et al.* 1986; Bachiller & Cernicharo 1986; Langer *et al.* 1989; Dickman & Herbst 1990; Lada *et al.* 1994).

To estimate differential extinction along the optical outflows, we performed star counts on the POSS plates. We selected four $\sim 3' \times 3'$ areas roughly centered at the positions of knots B, D, the centroid of knots E's, and a field or control area centered at $\alpha(2000.0) = 20^{\text{h}}46^{\text{m}}55^{\text{s}}$, $\delta(2000.0) = 68^\circ 05' 30''$. The region around knot B has practically no extinction compared to the field region. We estimate ~ 3 mag of differential extinction between the area centered on knots D and B and ~ 1.5 mag between the area around our most southern [S II] knots (the E knots) and the region around knot B. Consequently, there is a gradient in the density of the cloud along the SE optical flow that goes from ~ 5 mag at the position of the counter-fan nebula and the red ^{13}CO lobe (Levreault & Opal 1987; Levreault 1984) to 1.5 mag at the position of knots E's.

The [S II] flow, HH 315, shows a clear S-shaped morphology that can be produced by a slowly precessing jet with opening angle of $\sim 45^\circ$ and precession period of ~ 8300 yr,

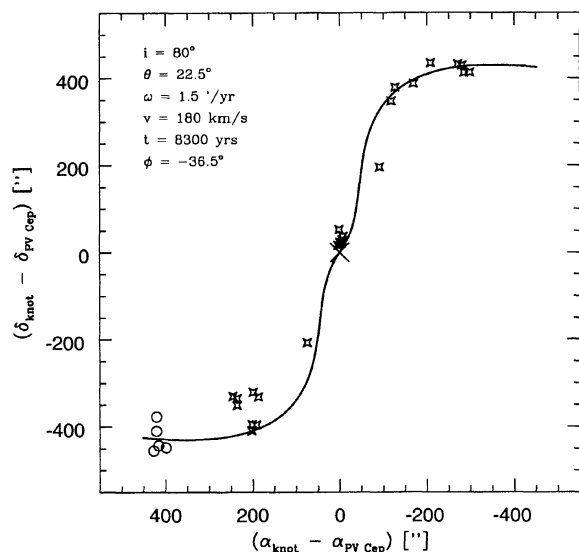


FIG. 6. The starred symbols indicate the offset positions of the HH knots (listed in Table 2) with respect to the central star (the cross). The open circles correspond to the offset positions of knots F1–5 provided by Dr. Bo Reipurth (see Reipurth *et al.* 1997). The solid line shows the precessing helical optical outflow for the parameters listed in the upper-right corner, where i is the inclination to the line of sight.

assuming a standard jet velocity of $\sim 200 \text{ km s}^{-1}$. The jet axis practically coincides with the plane of the sky ($i \sim 80^\circ$) and is almost perfectly aligned with the axes of the reflection nebula and the molecular outflows. The precessing jet carves a broad cavity in the envelope that is consistent with the opening angle of the reflection nebula and the opening angle estimated from near-IR line profiles (Hamann *et al.* 1994). The northern lobe is composed of several major [S II] condensations and a number of minor individual knots [see Fig. 5(a)]. The position angle of the consecutive major [S II] condensations change by a few degrees while the minor emissions roughly lie along the same direction.

The complex image morphology of HH 315 clearly suggests that the jet direction of ejection changes with time. The precessing jet axis model provides a simple prescription for a time-dependent direction of ejection that reproduces the overall shape of the PV Cep [S II] emission. However, less regular or constrain jet axis motion such as “wobbling,” “wiggling,” or “twisting” may also account for the HH 315 image morphology as well.

Mundt & Ray (1994) listed a dozen Herbig Ae/Be stars associated with optical outflows. The flows lengths typically range from ~ 0.1 to ~ 0.6 pc. Only one star, R Mon, has a parsec scale jet (~ 2 pc; cf. Walsh & Malin 1985; Schwartz & Schultz 1992). Therefore, PV Cep is one of the few Herbig Ae/Be stars known to drive a large-scale optical outflow.

In many young stars, the presence of several distinct clusters of [S II] emission knots has been related with multiple FU Orionis eruptions of the central object. In this interpretation, the accretion rate from the disk onto the central star periodically increases by factors of 100–1000. The mass loss rate also increases and this “extra” mass loss can have an

important impact on the surrounding cloud. Over a series of eruptions, a significant amount of mass and momentum can flow to the parental cloud and power the optical jet/molecular outflow phenomenon. If optical jets do arise from FU Ori events, the [S II] images then provide a “historical” record of previous eruptions (Dopita 1978; Königl 1982; Pringle 1989; Reipurth 1989; Hartigan *et al.* 1990; Reipurth & Heathcote 1991; Reipurth *et al.* 1992; Hartmann *et al.* 1993b; Kenyon *et al.* 1993; Reipurth & Cernicharo 1995; Kenyon 1995; Hartmann & Kenyon 1996).

In this picture, the radial length of the HH knots provides an estimate of the outburst duration; the spacing between knots constrains the time between FU Ori eruptions. The relative distance, in the radial direction, between the major emission knots in the HH 315 optical flow is ~ 0.4 pc (see Table 2) and ~ 0.02 pc among the individual knots. This knotty structure suggests a situation in which the jet axis precesses from one major eruption to the next and maybe nutates between minor eruptions. For example, knot B, with several nested contours and individual blobs of emission lying roughly in the same direction, has an internal structure that might indicate some nutation [see Fig. 5(a)]. If we adopt a jet velocity of $\sim 200 \text{ km s}^{-1}$, major eruptions need to occur every ~ 2000 yr. Minor eruptions then occur every ~ 100 yr. FU Ori objects have (or are expected to have) periods on time scale of a few decades to more than a thousand years (cf. Hartmann *et al.* 1993b; Hartmann & Kenyon 1996) in rough agreement with the interval between eruptions as suggested by the spacing among PV Cep [S II] knots.

Finally, the PV Cep optical outflow (HH 315) resembles the superjet associated with HH 34 in Orion A. Bally & Devine (1994) suggest that the 15–20 HH knots in a $23'$ field centered on the relatively low luminosity ($\sim 28 L_\odot$) embedded source (HH 34) outline a remarkably long, 3 pc, optical outflow. Bally & Devine identify a quasi-periodic separation among the HH knots that can be produced by a sequence of episodic mass-loss events from the central star. The HH 34 optical flow also shows an S-shaped morphology that could result from jet precession with a period of $\sim 10^4$ yrs. PV Cep has a higher luminosity, $\sim 80 L_\odot$ (Wilking 1983, quoted by Leveault 1984), and drives a somewhat shorter ~ 2.3 pc long optical jet, but otherwise closely resembles the HH 34 jet. These jets and other long or precessing jets (e.g., HH 366 and HH 333, Bally *et al.* 1996a, 1996b) have relied on the recent availability of large format CCD imagers. These discoveries suggest that long, precessing jets may be a more common feature of star formation than previously thought.

We are grateful to the staff at FLWO, specially to Perry Berlind, Ted Groner, Jim Peters, and Bas van't Sant. We thank Dr. John Raymond for lending us the [S II] and continuum nearby filters we used to observe PV Cephei. Special thanks to Dr. Bo Reipurth, the referee, for comments and suggestions that improved the paper. Dr. Reipurth also provided the coordinates of knots F1–5 and the HH 315 nomenclature in advance of publication. This research was supported by NASA Grant (NAGW-2919). M. G. acknowledges partial supports from the CONICOR (Argentina) through the

AIF grants for young researches and by the National Science Foundation through Grant GF-1001-96 from the Association of Universities for Research in Astronomy, Inc. under NSF cooperative agreement AST-8947990. IRAF is distributed by

the National Optical Astronomy Observatories, which is operated by the Association of Universities for Research in Astronomy, Inc., under contract to the National Science Foundation.

REFERENCES

- Adams, F. C., & Lin, D. N. 1993, *Protostars and Planets III*, edited by E. H. Levy and J. I. Lunine (Tucson University of Arizona, Arizona), p. 721
- Anglada, G., Rodríguez, L. F., Cantó, J., Estalella, R., Torrelles, J. M. 1992, *ApJ*, 395, 494
- Bachiller, R., & Cernicharo, J. 1986, *ApJ*, 166, 283
- Bally, J., & Devine, D. 1994, *ApJL*, 428, 65
- Bally, J., Devine, D., & Alten, V. 1996a, *ApJ*, 473, 921
- Bally, J., Devine, D., & Reipurth, B. 1996b, *ApJL*, 473, 49
- Bally, J., Devine, D., Fesen, R. A., & Lane, A. P. 1995, *ApJ*, 454, 345
- Bastien, P., & Ménard, F. 1990, *ApJ*, 364, 232
- Biro, S., Raga, A. C., & Cantó, J. 1995, *MNRAS*, 275, 557
- Carr, J. S. 1990, *AJ*, 100, 1244
- Chernin, L. M., & Masson, C. R. 1995, *ApJ*, 455, 182
- Cohen, M. 1980, *AJ*, 85, 29
- Cohen, M., Kuhl, L. V., & Harlan, E. A. 1977, *ApJL*, 215, 127
- Cohen, M., Kuhl, L. V., Harlan, E. A., & Spinrad, H. 1981, *ApJ*, 245, 920
- Curiel, S., Moran, J. M., Rodríguez, L. F., & Cantó, J. 1994, *Ap&SS*, 216, 137
- Dickman, R. L. 1978, *ApJS*, 37, 407
- Dickman, R. L., & Herbst, W. 1990, *ApJ*, 357, 531
- Dopita, M. A. 1978, *A&A*, 63, 237
- Duvert, G., Cernicharo, J., & Baudry, A. 1986, *A&A*, 164, 349
- Frerking, M. A., William, D. L., & Wilson, R. W. 1982, *ApJ*, 262, 590
- Gledhill, T. M., Warren-Smith, R. F., & Scarrott, S. M. 1987, *MNRAS*, 229, 643
- Gómez, M., Whitney, B. A., & Kenyon, S. J. 1997, *AJ* (submitted)
- Greene, T. P., & Lada, C. J. 1996, *AJ*, 112, 2184
- Grower, A., Gregory, P. C., Hutchings, J. B., & Unruh, W. G. 1982, *ApJ*, 262, 496
- Gueth, F., Guilloteau, S., & Bachiller, R. 1996, *A&A*, 307, 891
- Gyul'budagyan, A. L., & Magakyan, T. Yu. 1977, *Pis'ma Astron. Zh.*, 3, 162
- Gyul'budagyan, A. L., Magakyan, T. Yu., & Amirkhanian, A. S. 1977, *Pis'ma Astron. Zh.*, 3, 113
- Hamann, F., & Persson, S. E. 1992a, *ApJS*, 82, 285
- Hamann, F., & Persson, S. E. 1992b, *ApJ*, 394, 628
- Hamann, F., Simon, M., Carr, J. S., & Prato, L. 1994, *ApJ*, 436, 292
- Hartigan, P., Raymond, J., & Meaburn, J. 1990, *ApJ*, 362, 624
- Hartmann, L., & Kenyon, S. J. 1996, *ARA&A*, 34, 207
- Hartmann, L., Kenyon, S. J., & Calvet, N. 1993a, *ApJ*, 407, 219
- Hartmann, L., Kenyon, S. J., & Hartigan, P. 1993b, in *Protostars and Planets III*, edited by E. H. Levy and J. I. Lunine (Tucson University of Arizona, Arizona), p. 497
- Herbig, G. H., & Bell, K. R. 1988, *Lick Obs. Bull.*, No. 1111
- Hodapp, K-W. 1994, *ApJS*, 94, 615
- Hjellming, R. M., & Johnston, K. J. 1981, *ApJL*, 246, 141
- Hollis, J. M., & Michalitsianos, A. G. 1993, *ApJ*, 411, 235
- Kenyon, S. J. 1995, in *Revista Mexicana de Astronomía y Astrofísica, Serie de Conferencias*, Vol. 1, p. 237
- Kenyon, S. J., Hartmann, L., Gómez, M., Carr, J. S., & Tokunaga, A. 1993, *AJ*, 105, 1505
- Königl, A. 1982, *ApJ*, 261, 115
- Königl, A., & Ruden, S. P. 1993, in *Protostars and Planets III*, edited by E. H. Levy and J. I. Lunine (Tucson University of Arizona, Arizona), p. 641
- Lada, C. J., Lada, E. A., Clemens, D. P., & Bally, J. 1994, *ApJ*, 429, 694
- Langer, W. D., Wilson, R. W., Goldsmith, P. F., & Beichman, C. A. 1989, *ApJ*, 337, 355
- Levreault, R. M. 1984, *ApJ*, 277, 634
- Levreault, R. M. 1988, *ApJ*, 330, 897
- Levreault, R. M., & Opal, C. B. 1987, *AJ*, 93, 669
- Lightfoot, J. F., & Glencross, W. M. 1986, *MNRAS*, 221, 993
- Lin, W., Evans II, N. J., Harvey, P. M., & Colomé, C. 1994, *ApJ*, 433, 199
- Martí, J., Rodríguez, L. F., & Reipurth, B. 1993, *ApJ*, 416, 208
- Masson, C. R., & Chernin, L. M. 1993, *ApJ*, 414, 230
- Mundt, R., & Ray, T. 1994, in *The Nature and Evolutionary Status of Herbig Ae/Be Stars*, *APS Conf. Ser.* 62 edited by P. S. Thé, M. R. Pérez, and E. P. J. van den Heuvel (ASP, San Francisco), p. 237
- Neckel, T., & Staude, H. J. 1984, *A&A*, 131, 200
- Neckel, T., Staude, H. J., Sarcander, M., & Birkle, K. 1987, *A&A*, 175, 231
- Pringle, J. E. 1989, *MNRAS*, 236, 107
- Raga, A. C., & Biro, S. 1993, *MNRAS*, 264, 758
- Raga, A. C., & Cabrit, S. 1993, *A&A*, 278, 267
- Raga, A. C., Cantó, J., Calvet, N., Rodríguez, L. F., & Torrelles, J. M. 1993a, *A&A*, 276, 539
- Raga, A. C., Cantó, J., & Biro, S. 1993b, *MNRAS*, 260, 163
- Ray, T. P. 1994, *Ap&SS*, 216, 71
- Reipurth, B. 1989, in *Low-Mass Star Formation and Pre-Main-Sequences Objects*, edited by B. Reipurth (ESO, Garching), p. 247
- Reipurth, B. 1994, *A General Catalogue of Herbig-Haro Objects*, electronically published via anonymous ftp to ftp.hq.eso.org, directory /pub/Catalogs/Herbig-Haro
- Reipurth, B., & Cernicharo, J. 1995, in *Revista Mexicana de Astronomía y Astrofísica, Serie de Conferencias*, Vol. 1, p. 43
- Reipurth, B., & Heathcote, S. 1991, *A&A*, 246, 511
- Reipurth, B., & Heathcote, S. 1992, *A&A*, 257, 693
- Reipurth, B., Bally, J., & Devine, D. 1997 (unpublished)
- Reipurth, B., Raga, A. C., & Heathcote, S. 1992, *ApJ*, 392, 145
- Savage, B. D., & Mathis, J. S. 1979, *ARA&A*, 17, 73
- Scarrott, S. M., Rolph, C. D., & Tadhunter, C. N. 1991, *MNRAS*, 249, 131
- Scarrott, S. M., Warren-Smith, R. F., Draper, P. W., & Gledhill, T. M. 1986, *Can. J. Phys.*, 64, 426
- Schwartz, R. D., & Schultz, A. S. B. 1992, *AJ*, 104, 220
- Stahler, S. 1994, *ApJ*, 422, 616
- Thé, P. S., de Winter, D., & Pérez, M. R. 1994, *A&AS*, 104, 315
- Walsh, J. R., & Malin, D. F. 1985, *MNRAS*, 217, 31

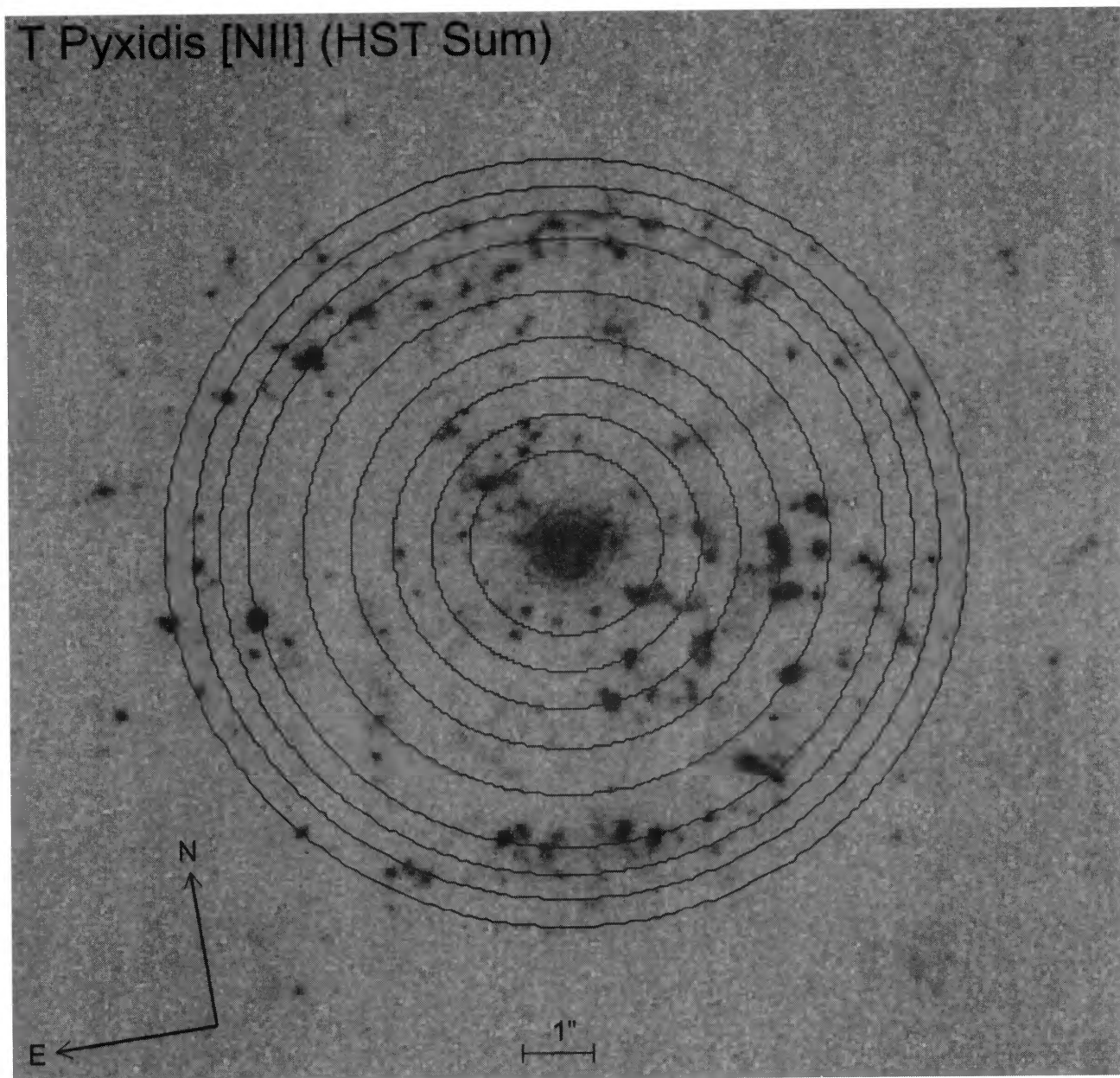


FIG. 15. Summed [N II] *HST* image with the positions of the peaks in Fig. 14 overlaid.

Shara et al. (see page 262)

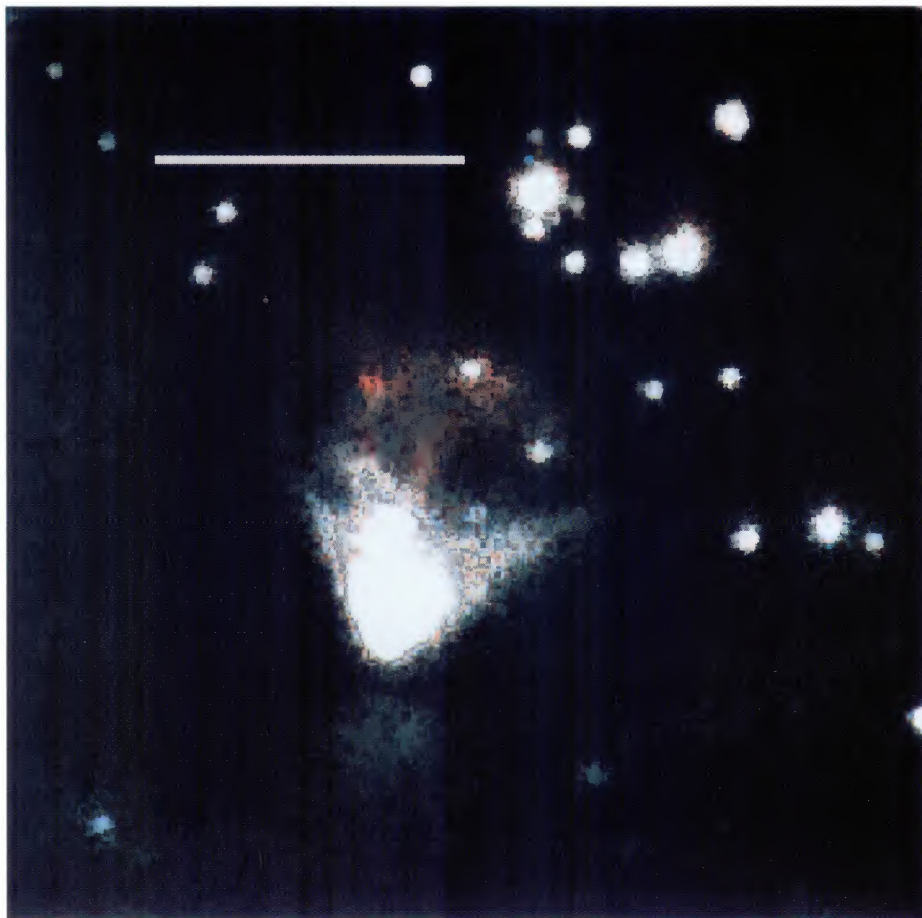


FIG. 2. Three-color image of PV Cep for the combined (1993 and 1994) date covering a field of view of $\sim 3' \times 3'$. The [S II] image is red, and the nearby continuum is assigned to the green and blue planes. The white bar shows a scale of $1'$. North is up and east is left.

Gomez *et al.* (see page 266)